

## Article

# Effect of Microstructure and Mechanical Properties of Al5083 Alloy Processed by ECAP at Room Temperature and High Temperature

Muneer Baig <sup>1,2</sup>, Ateekh Ur Rehman <sup>3</sup>, Jabair A. Mohammed <sup>2</sup> and Asiful H. Seikh <sup>2,\*</sup>

<sup>1</sup> Engineering Management Department, College of Engineering, Prince Sultan University, P.O. Box 66833, Riyadh 12435, Saudi Arabia; mbaig@psu.edu.sa

<sup>2</sup> Centre of Excellence for Research in Engineering Materials, Deanship of Scientific Research, King Saud University, P.O. Box 800, Riyadh 11421, Saudi Arabia; jmohammed@KSU.EDU.SA

<sup>3</sup> Department of Industrial Engineering, College of Engineering, King Saud University, P.O. Box 800, Riyadh 11421, Saudi Arabia; arehman@ksu.edu.sa

\* Correspondence: aseikh@ksu.edu.sa



**Citation:** Baig, M.; Rehman, A.U.; Mohammed, J.A.; Seikh, A.H. Effect of Microstructure and Mechanical Properties of Al5083 Alloy Processed by ECAP at Room Temperature and High Temperature. *Crystals* **2021**, *11*, 683. <https://doi.org/10.3390/cryst11060683>

Academic Editors: Assem Barakat and Alexander S. Novikov

Received: 29 May 2021

Accepted: 11 June 2021

Published: 14 June 2021

**Publisher's Note:** MDPI stays neutral with regard to jurisdictional claims in published maps and institutional affiliations.



**Copyright:** © 2021 by the authors. Licensee MDPI, Basel, Switzerland. This article is an open access article distributed under the terms and conditions of the Creative Commons Attribution (CC BY) license (<https://creativecommons.org/licenses/by/4.0/>).

**Abstract:** In this investigation, the focus is on improving the quality of the Al 5083 alloy by equal-channel angular pressing (ECAP) innovation. Equal-channel angular pressing (ECAP) is one of the best technologies for converting macro grain into ultra-fine-grained structure. Grain structure which is finer increases the strength of the material. In this work, a severe plastic deformation using equal-channel angular pressing (ECAP) up to 3 passes was given on Al5083 alloy using path B<sub>C</sub> at room temperature. The evolution of the microstructure was studied using an optical microscope. Tensile studies were also done. Both hardness (Vickers) and tensile strength rises as the number of passes increases; however, the ductility or the percentage of elongation increases. It can be said that the final product of this aforementioned alloy after ECAPed processing is considered to be suitable for various applications in which higher strength is required.

**Keywords:** ECAP; Al5083 alloy; ultra-fine grain; hardness; tensile strength

## 1. Introduction

In different design applications, aluminum and its alloys are generally used as the most frequent or common material. The interest in ultra-fine-grained aluminum 5083 alloy has expanded greatly as it has high strength, great weldability, and corrosion resistance. These properties are required in the field of vehicle bodies, shipbuilding, pressure vessels, and armor plates, and therefore the use of this alloy in these fields has increased. Researchers are trying to develop high-strength materials that possess ultra-fine grain (UFG) using various severe plastic deformation (SPD) methods.

Equal-channel angular pressing (ECAP) is one of the most important SPD methods. In this technique, the subjects are cast out with no adjustment to the cross-segment by exposing them to enormous shear strain. The preparation technique for ECAP incorporates the squeezing of a billet using a die comprising 2 channels of equivalent cross-segment converging at a definite angle ( $\Phi$ ). A high shear strain is forced on the material while it goes through the shear zone of the die [1–3]. As the billet material has almost a similar cross-area during ECAP, it can be squeezed using the die repeatedly for additional passes. The route through which the deformation is given to the billet can be varied by changing the rotation of billet in the direction of 0° known as route A. The B<sub>A</sub> route is the alternate direction at an angle of 90°, B<sub>C</sub> is the same direction at an angle of 90°, and finally route C is at an angle of 180° [4]. By choosing the correct or suitable channel angle ( $\Phi$ ), the route by which deformation is given, i.e., route A or route B<sub>A</sub>, route B<sub>C</sub>, or route C, and the how many times the passes are given determines or controls the properties of microstructures as well as the strain exerted on the material [4–6]. Figure 1 demonstrate the four routes of

ECAP passes schematically. These routes create different slip systems during the pressing operation so that various microstructural and mechanical properties can be achieved [6].

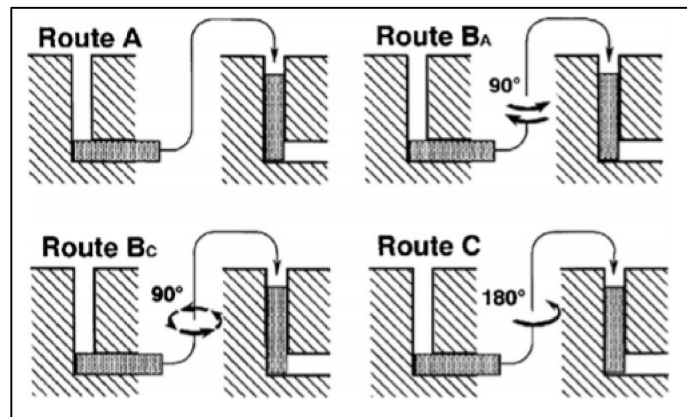


**Figure 1.** Four routes in the ECAP process.

Broad examination has been done on ECAP for as long as 20 years for the preparation of materials such as aluminum alloys [7–18], titanium [10,12], silver [13,15,17], magnesium [14], steel [10–15], chromium [18], and copper [7,10,14]. For the prepared material, mechanical and wear properties were discovered to be high, making ECAP a significant method for processing mass materials [10–14].

In this study, commercially available aluminum alloy (Al 5083) has been exposed to ECAP through route C at room temperature, improving the quality. The chemical composition of Al 5083 alloy is (Si-0.4, Fe-0.4, Cu-0.1, Mn-0.4-1.0, Mg-4.0-4.9, Zn-0.25, Ti-0.15, Cr-0.05-0.25, Al-Balance) percentage, and it is tested practically using mass spectroscopy method. Further examinations have been done on the microstructural and mechanical properties of the as-received and ECAPed compound.

## 2. Experimental Procedure

### 2.1. ECAP Process of Al 5083 Alloy

The specimens were pressed up to 3 passes (one, two, three) with the help of a hydraulic press (200 tons). This process was done at ambient temperature. In the present study, route C was employed for pressing (Figure 2 shown below) and a 0.6 mm/s pressing speed was maintained during this process. Several studies demonstrate that greater uniformity in the plastic strain induced in the ECAP cycle will be acquired using route C [19].

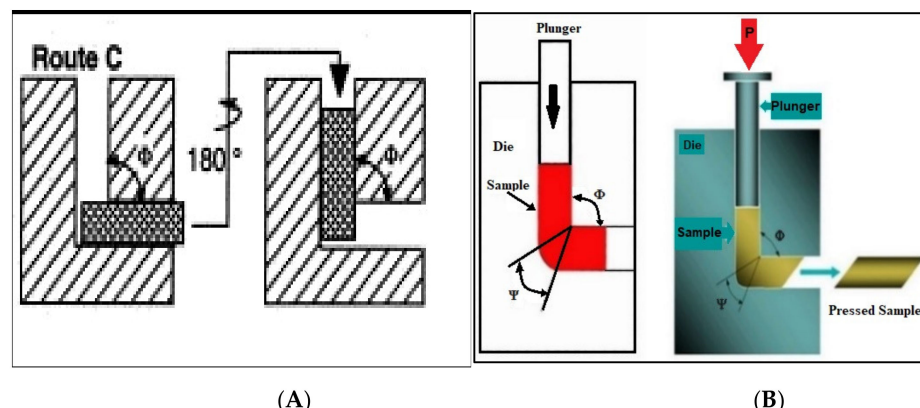


**Figure 2.** A schematic diagram of equal-channel angular pressing (ECAP) die: (A) route C path, (B) three-dimensional (3D) presentation of ECAP die.

## 2.2. Tensile Testing of ECAPed Samples

Here, the tensile samples are taken in the form of cylinder. Proper surface polishing was done. The gauge length of the specimen was 20 mm, whereas the diameter was 6.5 mm. These specimens were fabricated in this shape after the ECAP processing, as shown in Figure 3. Tensile tests were done at room temperature ( $\sim 28^{\circ}\text{C}$ ) until complete breakdown occurred. The testing equipment consisted of servo hydraulic power, which is controlled by a PC. Instron 8500 (R) of  $\pm 100$  kN load limit, using machine-dedicated tensile testing software, and Instron Bluehill tests were done under strain-control mode at a strain rate of  $10^{-3} \text{ s}^{-1}$  using an extensometer of 25 mm gauge length.

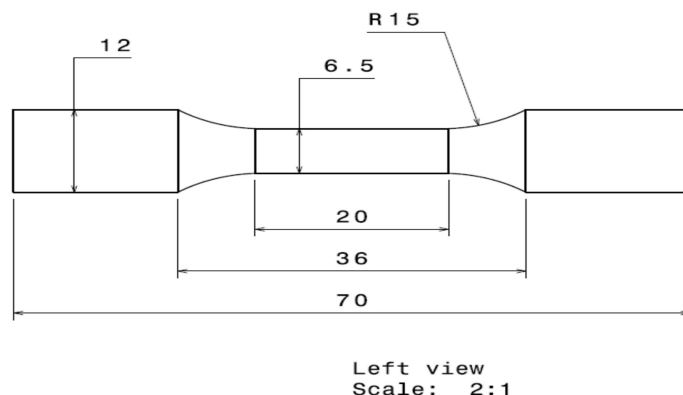


**Figure 3.** Dimensions of the sample prepared for the tensile test.

## 2.3. Optical Microstructure

Different grades of emery paper were used to polish the specimens properly. Furthermore, the samples were polished in a cloth polisher with the help of abrasives such as alumina. Ultrasonic cleaner was used to obtain a clear surface. Keller's (190 mL  $\text{H}_2\text{O}$  + 5 mL  $\text{HNO}_3$  (65%) + 3 mL HCl (32%) + 2 mL HF (40%)) reagent was used as etchant [20]. Microstructural analysis of these samples was examined under a Leica optical microscope.

## 2.4. Hardness

Microhardness of the samples during ECAP processing was estimated along the transverse plane using a Vickers microhardness analyzer. In this process, a 100 gm load for 20 s was applied.

## 3. Results and Discussions

### 3.1. Microstructure

Optical micrographs of untreated and ECAPed specimens are given in Figure 4a–d. The alloy without the ECAP, i.e., as-received alloy, shows coarse grain structure. At the point when the size of the grain decreases to one or a few microns, intragranular distortion will prevail and intergranular distortion, which includes slipping, dislocation and twinning, will be stifled somewhat. The microstructures demonstrate the fact that with high deformation degree, microscopically homogeneous fine-grained structures are formed. The as-received sample shows the size of grain to be 145  $\mu\text{m}$ . From there, it decreases to 37  $\mu\text{m}$  after the 3rd pass, and grain size is measured by ImageJ software. After doing ECAP, there was a remarkable increase in the tensile property, which was reported by several studies [21,22]. The refinement of grain actually occurs due to the ECAP process, which causes deformation in the material.

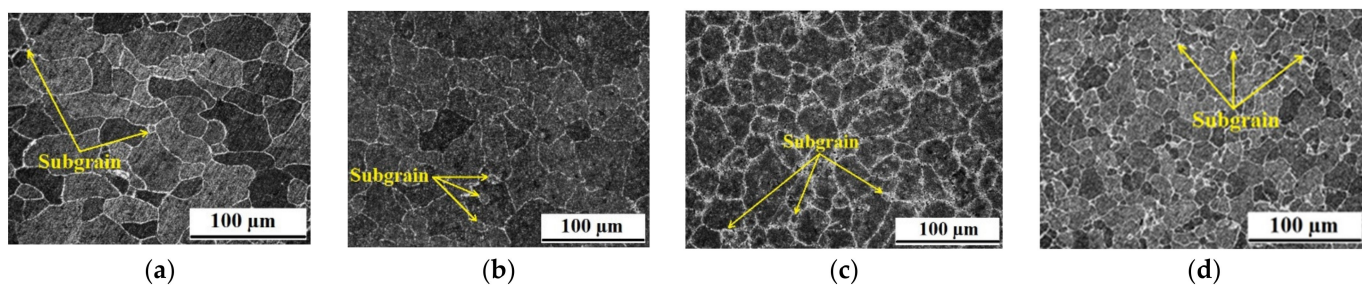


**Figure 4.** Microstructure of Al5083 alloy of (a) annealed and ECAP after (b) 1st pass, (c) 2nd pass, and (d) 3rd pass.

In terms of cross-section, the size of the grain decreases and the same is increased in terms of the longitudinal section. The refinement of grain, as well as the elongation of the specimens, are given in Figure 4. After the first pass, the actual grains divided into sub-grain bands and thus the primary size of the grain is reduced.

Another thing that should be emphasized is that the stress-strain curve of the three-pass specimen exhibits a steady-state flow behavior without strain-solidifying subsequent to yielding. The characteristics are primarily connected to the microstructure that is treated with the ECAP process. On account of the multi-pass ECAP, for the first pass of ECAP, the speed of dislocation increase is a lot bigger than that of the dislocation obliteration, because of the low dislocation density. Along these lines, the grains of the material can be fundamentally refined. During further pass-pressing treatment, grain refinement proceeds in light of the fact that the dislocation density and the inner energy are expanded. However, the expansion of the internal energy causes crystalline recovery and recrystallization measures, so the refinement process of the grain slowly diminishes after a few passes of pressing. However, the grain refinement advancement cycle of the sample is changed for different pressing paths. The accumulation and equilibrium of the dislocations are likewise different for route C. Through examination of the deformation and dislocation advancement, it tends to be seen that the nanostructured materials can be obtained by ECAP method. The cycle of grain refinement can be shown as a constant dynamic recovery and recrystallization. From the perspective of microstructure investigation, the grain refinement method controls the dynamic equilibrium of the generation and annihilation of the dislocations [22].

### 3.2. Microhardness

Vickers (HV) microhardness was measured at room temperature before and after ECAP and the data are given in Table 1 and in Figure 5. From the data, it is quite clear that the value of hardness increases after ECAP processing, compared to the as-received sample, and it increases gradually as the pass increases.

**Table 1.** Microhardness value of Al5083 alloy before and after ECAP.

Sample	Vickers Microhardness (HV)	Errors
As received	70	±0.5
1st Pass	75	±0.47
2nd Pass	82	±0.31
3rd Pass	91	±0.21

From Figure 4, the percentage increment of microhardness from no pass to 3rd pass is approximately equal. This is due to the grain refinement and homogeneity of the structure of the alloy.

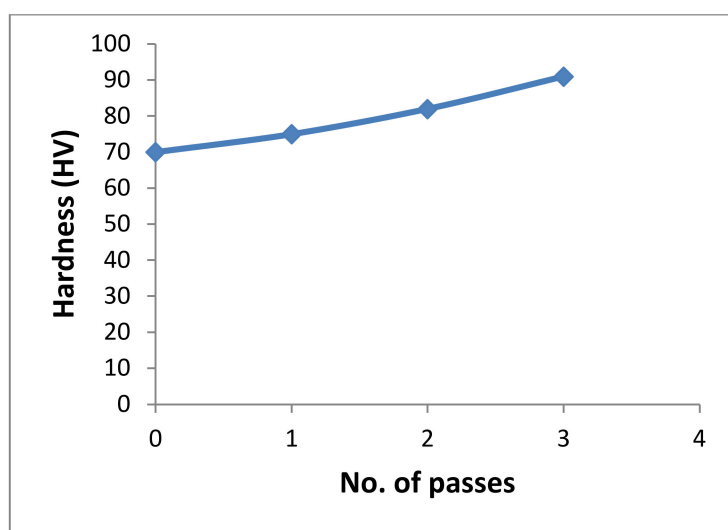


**Figure 5.** Vickers hardness of Al 5083 alloy before and after ECAP.

### 3.3. Tensile Properties

In Table 2, the details of the tensile properties of Al5083 alloy before and after ECAP are given. The no-pass sample, i.e., as-received alloy, exhibits the yield strength (YS), and the ultimate tensile strength (UTS) was 221 MPa and 303 MPa, with an elongation of 12.71%. As the passes increase, the YS and UTS value also increases gradually. In addition, after the 3rd pass, the UTS value of this sample increases to 336 MPa and the YS also increases to 294 MPa with an elongation of 3.92%. Though the value of strength of the alloy increases as the passes increase, the percentage of elongation decreases from 12.71% to 3.92%. The reason for this may be due to the processing of ECAP, and strain-hardening of materials occurred. It is inferred that the expansions in strength of the alloy preparation treatment using ECAP is chiefly because of grain refinement [23]. The grain size is phenomenally diminished and refined after one-pass ECAP. Furthermore, partition shows up in specific grains and grain boundary, and is improved accordingly. Additionally, twins likewise play a huge role in modifying the YS, which may act as a limit to disengagement slip and add to the improved properties. Therefore, it is the grain refinement and mix of twinning and separation that force to the extension of YS. It is obvious that prolongation is decreased after the essential pass. When in doubt, the malleability of materials for the most part diminishes after having been dealt with by twisting. The drop of expansion may be credited to the extraordinary plastic turning in metals, and the improvement of partitions cannot expect a section in refined microstructures, which can similarly be clarified as committed.

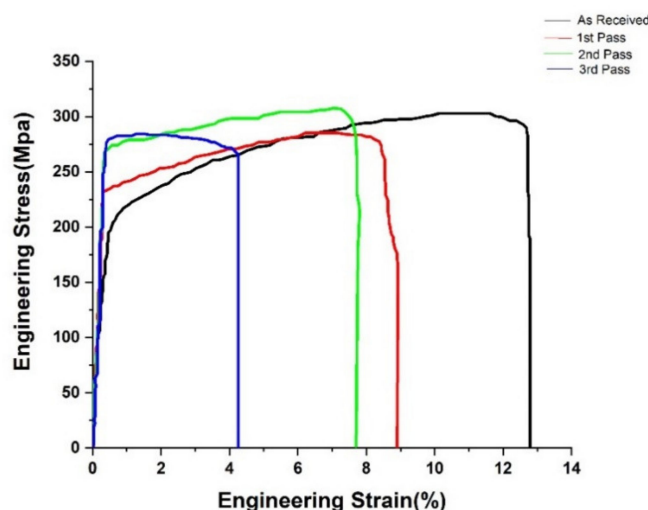
**Table 2.** Tensile properties of Al 5083 alloy before and after ECAP.

Specimen Condition	Yield Strength (MPa)	Errors	UTS (MPa)	Errors	Total Strain (%)	Errors
As received	221	±0.25	303	±0.20	12.71	±0.35
1st Pass	255	±0.23	305	±0.29	8.94	±0.32
2nd Pass	288	±0.31	327	±0.19	7.71	±0.21
3rd Pass	294	±0.20	336	±0.22	3.92	±0.12

In Table 3 and Figure 6, the details of tensile properties of Al5083 alloy before and after ECAP at high temperature, i.e., 250 °C, are given.

**Table 3.** High-Temperature Mechanical Properties of Al 5083 at 250 °C.

Specimen Condition	Yield Strength (MPa)	Errors	UTS (MPa)	Errors	Total Strain (%)	Errors
As Received	243	±0.125	257	±0.23	5.72	±0.17
First Pass	246	±0.25	261	±0.18	5.20	±0.19
Second Pass	249	±0.21	263	±0.156	4.89	±0.22
Third Pass	251	±0.15	265	±0.31	4.39	±0.12

**Figure 6.** The tensile curve of Al 5083 alloy in  $10^{-3}$ /s strain rates in ambient temperature.

The no-pass sample, i.e., the as-received alloy, exhibited the yield strength (YS), and ultimate tensile strength (UTS) was 243 MPa and 257 MPa with an elongation of 5.72%. As the passes increase, the YS and UTS value also increases gradually. In addition, after the 3rd pass, the UTS value of this sample increases to 265 MPa, and the YS also increases to 251 MPa with an elongation of 4.39%. Though the value of strength of the alloy increases as the passes increases, the percentage of elongation decreases from 5.72% to 4.39%. The reason behind this may be due to the processing of ECAP, and strain-hardening of materials occurred. In both the ambient temperature and high temperature, the YS and UTS of the alloy increases gradually, but in the case of high temperature, the rate of increment is a little slow. On the other hand, the percentage of elongation in both cases decreases gradually, while the rate is slow in the case of the high-temperature ECAPed sample.

Figures 6 and 7 exhibit the stress–strain curve and varieties of YS, UTS, and percentage of elongation of the treated samples of Al5083 alloy versus passes of the procedure at room temperature and at 250 °C.

From the given figure (Figures 6 and 7), it is clear that with expanding the quantity of passes of the ECAP cycle, tensile strength expanded while elongation diminished. However, the steady-state stream conduct can be additionally ascribed to the homogeneous spreading of the microstructure after the 3rd pass of ECAP. Thus, evident solidifying work vanished from the curve during the uniaxial compressive tests. The curve of the as-cast one shows a conspicuous yield point, and shows extremely low yield strength of about 243 MPa. With one-pass ECAP notwithstanding, it is not hard to find that the curve presents a particular strain solidification, and YS is fundamentally improved with an estimation of 246 MPa. Concerning the expansion of YS, it is steady with the exemplary Hall–Petch relationship, which explains that with grain size reduction, the improvement in YS of a polycrystalline material takes place. Varieties of strength of tensile properties of metals exposed to SPD could result from both underlying causes: work hardening by dislocations and refinement of grain [24], on account of the expanded density of dislocations, strain-hardening, use of enormous strains, and cold working. Towards the end of the 1st pass of the cycle,

YS and UTS expanded unexpectedly, while the rate of elongation dropped rapidly. The expansion of the strength in the resulting passes of the process was preliminarily a direct result of the structure of grain development (microstructural adjustment) as opposed to the arrangement of fine grains. In this way, the rates at which yield strength expanded and at which elongation was reduced were fundamentally lower, as contrasted with that of the 1st pass. Further expansion in strain solidification after the post-ECAP maturation is thought to have been dictated by three elements in rivalry: separation thickness decrease, and exhaustion of solutes in strong arrangement. The first and second factors should expand the strain-solidifying capacity, while the third factor diminishes it. Strain-solidifying will be improved during the maturation cycle as separation thickness is diminished because of the recuperation impact during maturing. Production of non-sharable acceleration during the maturation cycle will likewise build the strain solidification by permitting extra separation stockpiling by instigating disengagement circles around the particles. Exhaustion of solutes in strong arrangement during maturation, however, will decrease the capacity of the material to store a high thickness of disengagements by expanding the dynamic recuperation rate.

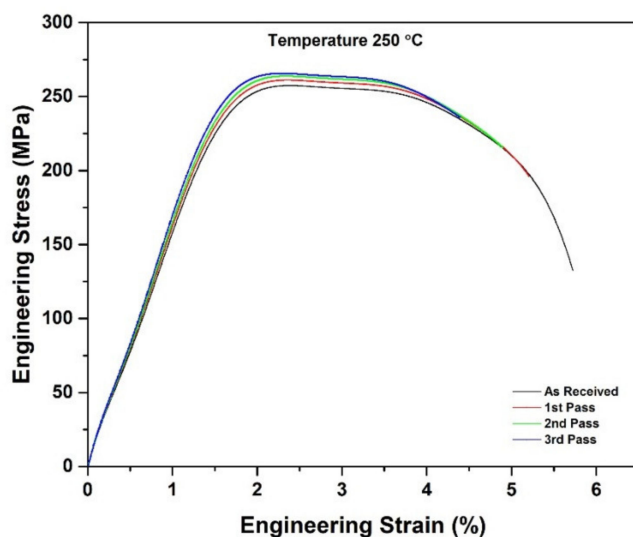


**Figure 7.** The tensile curve of Al 5083 alloy in  $10^{-3}/\text{s}$  strain rates in  $250\text{ }^{\circ}\text{C}$  temperature.

### 3.4. Fractography

The fractured surface morphology of the Al5083 alloy in an annealed state after ECAP is given in Figure 8. The fracture surface of the sample in as-received state after ECAP at high temperature is shown in Figure 9. The insufficiency of plasticity is denoted by several dimples present in the surface area of the untreated sample. The increment of stress concentration occurs due to the variation between the modulus of elasticity of the matters and the matrix [8]. When the size of the particles becomes large and their consistency at the boundary phase is lesser, then the formation of micro-cracks takes place with low plastic deformation. The morphology of the surface comprises a various arrangement of holes (dimples) of varying sizes and shapes, framed in the region of the particles of the scattered stage. The fractography of the break surface demonstrates that the breaks will in general go through eutectic mixes. Obviously, this is a weak crack. In a weak break, breaks may spread quickly, with little plastic deformation.

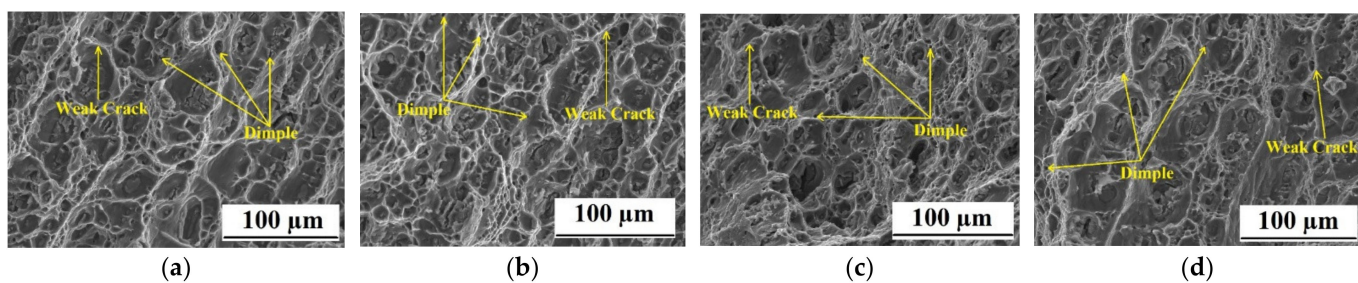


**Figure 8.** The ambient temperature tensile fracture surfaces of the sample after surface of the 5083 alloy of (a) annealed and ECAP after (b) 1st pass (c) 2nd pass and (d) 3rd pass.

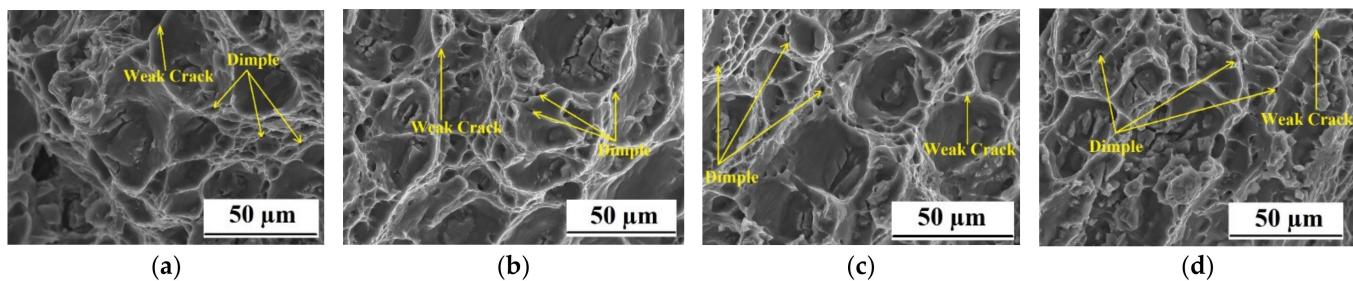


**Figure 9.** The 250 °C temperature tensile fracture surfaces of the sample after surface of the 5083 alloy of (a) annealed and ECAP after (b) 1st pass (c) 2nd pass, and (d) 3rd pass.

Fracture cross-segments of the annealed samples, similar to those that went through the die in ECAP for an alternate number of passes, were researched using Scanning electroc microscopy (SEM) following tensile testing. Predominant failure components in the metals with the side-captured cubic crystal structure are cavity arrangement followed by soft failure. Generally, ductile cracking happens as coaxial or hemispherical dimples. This sort of failure occurred with the arrangement of microcavities, integration, crack propagation, and afterwards shear failure along a direction near that of tension (Figure 8). This is because in the Al–Si combination, porosity, particles/lattice interface, and sharp edges of particles are the expected locales for break inception because these are the pressure risers. It should be noticed that the method of break is identified with the system of crack propagation.

Considering Figure 8a–d, with a growing number of passes of the ECAP interaction, the microcavities become more modest and shallower diverged from the strengthened example. The presence of these miniature cavities in the break surfaces of the ECAPed tests proposes the occurrences of the typical shear pliable crack system as in the underlying example, as miniature holes become more modest and shallower, causing extended elasticity and lessened lengthening in contrast with the underlying example [9]. The presence of shallower and more modest holes implies shear malleable breaking, which resembles the disappointment in the underlying example, with the primary differentiation being the shallower profundity of the breaks for the present circumstance. This could be interpreted as higher rigidity, and consequently, a lower extension rate in the examples went through the pass-on, as demonstrated differently in relation to the underlying (strengthened) example. The disappointment surfaces of the underlying and ECAPed materials (Figure 8) show some hemispheroidal and miniature depressions, and some miniature holes are flowing in one or alternate routes because of the application of inconsistent triaxial stresses. These dimples are the features of a commonplace malleable break [4]. Each miniature hole is attributed to a break nucleation site, which is associated with the plastic misshaping cycle [25].

Expanding the quantity of leave-behinds to 2, the number of broken small cell and, furthermore, dimples (as shown by white circle) expanded. Unmistakably, a few locales of the break surface do not have any dimples. As per the stress–strain bend and the

presence of both weak highlights and dimples, it very well may be inferred that the crack mode is blended (for example a blend of both fragile and pliable break). The crack surface of the three ECAP passes show an enormous number of miniature dimples. The break surface of the three ECAP passes is filled by dimples with various sizes. Unmistakably, the component of the break is changed to a flexible crack. The flexible break is determined by wide plastic twisting in the region of a propelling break. A significant quality of this crack sort is the presence of dimples or miniature voids on the break surface. The presence of countless dimples and, furthermore, the fine circle prompted the achievement of the best pliable properties after the 3rd ECAP pass. The 3rd ECAP pass prompts extraordinary harm with a few slip follows and breaks. It can likewise be seen that, with expanding number of passes and diminishing size, the uniform round dimples are framed. Indeed, countless little dimples demonstrate a total pliable crack in the aluminum matrix. A cautious and exhaustive assessment of the tensile fractured surfaces gives helpful data on the particular function of characteristic microstructural impacts on strength and ductility properties. A cautious perception of the fracture surfaces revealed minute contrasts in general fracture morphology at the macroscopic level and characteristic fracture features. Figure 9a–c exhibit the fractography of the specimens that are treated with tensile. At the normally noticeable level, a malleable break of the examples was fundamentally ordinary to the pressure pivot. The overall morphology of the crack was unforgiving, uncovering areas of locally moldable and weak disappointment of the constituent particles. Higher amplification perceptions of the pliable break surfaces uncovered tiny breaking along the recrystallized grain limits. An assortment of particularly fine small breaks was clear along the recrystallized grain limits, reminiscent of locally fragile disappointment instruments. Trans-granular break districts saw are a direct result of the presence of the little second-stage particles, which causes the development of pockets of shallow dimples and infinitesimal voids of changing size [12]. Coarse constituent particles apparently had break/de-union from the grid beginning at the miniature voids. Discretionary breaks were similarly observed. The staggering component of disappointment has been viewed as miniature void nucleation, improvement, and mixture.

In both the directions, similar highlights have been noticed. Regular features of bendable break, delivered by the nucleation of dimples overwhelmingly from the coarse intermetallic particles, broke in a fragile way as shown in Figure 8. The fractured surfaces that are nucleated from the 2nd-phase particles of CuAl<sub>2</sub> show dimples [26].

At higher amplification, there are two sizes of dimples observed. The size range of 10–30 Pm of the dimples is the main population, and that is related to the cracks present in the 2nd-phase coarse particles [27]. Other sizes of dimples have been discovered to be finer in size (0.6–3 Pm) and shape because of the arrangement of ligament breaking between primary voids, causing shear voiding between the primary voids [28]. Similar features were found in all ageing conditions.

The Al framework surrounding the molecule was intensely twisted, and another miniature void populace was seen in the grid. It is imperative that such a quality of crack mode is correspondingly noticed, paying little mind to twisting temperature from room temperature to 250 °C or 523 K. In any case, it was additionally critical that the dimples of high disfigurement temperature were more profound and bigger than those shaped at ambient temperature.

#### 4. Conclusions

ECAP has been done on the Al5083 alloy to improve the quality of the sample. The exceptionally fine and uniform microstructure is obtained a coarse grain structure of untreated alloy after ECAP processing using route B<sub>C</sub>. As the pass number increases, the microhardness of the sample increases rapidly, and the reach in value of 91 HV after processing trough ECAP of up to 3 passes is due to the formation of fine grains. The YS and UTS, i.e., overall strength, increases with the increases of pass number and at the same time the ductility decreases due to the hardening of the specimen. It is concluded that the

mechanical properties of aluminum 5083 alloy are upgraded using ECAP treatment. The improvement of the mechanical properties of the alloy made it feasible to use the specimen in different design applications where higher strength is required. The consequences of this examination are as follows:

- (1) Complete elimination of the dendritic structure of the untreated Al5083 alloy, reduction in the size of grain, i.e., grain refinement, and uniform spreading of particles in the Al matrix is caused by processing through ECAP.
- (2) The maximum YS and UTS values were obtained after a third pass of the ECAP process. This improvement of strength is due to the refinement of the grain, uniform distribution of particles, and intermetallic compounds.
- (3) The mechanism of fracture is changed from brittle to ductile with an increasing number of passes of ECAP processing.
- (4) The nature of Al5083 alloy after the 3rd ECAP pass turned to a ductile fracture. Compared to the untreated sample, the sample after the 3rd pass of ECAP demonstrates much fewer stress concentration sites.

**Author Contributions:** Conceptualization, A.H.S., M.B., J.A.M., A.U.R.; Data curation, A.H.S., M.B., J.A.M., A.U.R.; Formal analysis, A.H.S., M.B., A.U.R.; Funding acquisition, A.H.S.; Investigation, A.H.S., J.A.M. and M.B.; Methodology A.H.S., M.B., J.A.M., A.U.R.; Resources, A.U.R.; Supervision, A.H.S., M.B., A.U.R.; Writing—original draft, A.H.S., J.A.M., M.B., A.U.R.; Writing—review and editing, A.H.S., M.B., A.U.R. All authors have read and agreed to the published version of the manuscript.

**Funding:** This project was supported by the NSTIP Strategic Technologies Program, grant number (12-ADV3109-02), Kingdom of Saudi Arabia.

**Institutional Review Board Statement:** Not applicable.

**Informed Consent Statement:** Not applicable.

**Data Availability Statement:** The experimental datasets obtained from this research work and then the analyzed results during the current study are available from the corresponding author on reasonable request.

**Acknowledgments:** This project was supported by the NSTIP Strategic Technologies Program, grant number (12-ADV3109-02), Kingdom of Saudi Arabia.

**Conflicts of Interest:** The authors declare no conflict of interest.

## References

1. Segal, V.M. Materials processing by simple shear. *Mater. Sci. Eng. A* **1995**, *197*, 157–164. [[CrossRef](#)]
2. Valiev, R.Z. Structure and mechanical properties of ultrafine-grained metals. *Mater. Sci. Eng. A* **1997**, *234–236*, 59–66. [[CrossRef](#)]
3. Valiev, R.Z.; Korznikov, A.V.; Mulyukov, R.R. Structure and Properties of Ultrafine-Grained Materials Produced by Severe Plastic Deformation. *Mater. Sci. Eng. A* **1993**, *168*, 141–148. [[CrossRef](#)]
4. Valiev, R.Z.; Langdon, T.G. Principles of equal-channel angular pressing as a processing tool for grain refinement. *Prog. Mater. Sci.* **2006**, *51*, 881–981. [[CrossRef](#)]
5. Sun, P.L.; Kao, P.W.; Chang, C.P. Effect of Deformation Route on Microstructural Development in Aluminum Processed by Equal Channel Angular Extrusion. *Met. Mater. Trans. A* **2004**, *35*, 1359–1368. [[CrossRef](#)]
6. Jianqiang, B.I.; Kangning, S.U.N.; Rui, L.I.U.; Runhua, F.A.N.; Sumei, W.A.N.G. Effect of ECAP Pass Number on Mechanical Properties of 2A12 Al Alloy. *J. Wuhan Univ. Technol. Mater. Sci. Ed.* **2008**, *71*–73.
7. Gao, L.; Cheng, X. Microstructure and mechanical properties of Cu–10%Al–4%Fe alloy produced by equal channel angular extrusion. *Mater. Des.* **2008**, *29*, 904–908. [[CrossRef](#)]
8. Khan, Z.A.; Chakkingal, U.; Venugopal, P. Analysis of forming loads, microstructure development and mechanical property evolution during equal channel angular extrusion of a commercial grade aluminum alloy. *J. Mater. Process. Technol.* **2003**, *135*, 59–67. [[CrossRef](#)]
9. Kucukomeroglu, T. Effect of equal-channel angular extrusion on mechanical and wear properties of eutectic Al–12Si alloy. *Mater. Des.* **2010**, *31*, 782–789. [[CrossRef](#)]
10. Gao, L.L.; Cheng, X.H. Microstructure and dry sliding wear behavior of Cu 10%Al–4%Fe alloy produced by equal channel angular extrusion. *Wear* **2008**, *265*, 986–991. [[CrossRef](#)]
11. Jufu, J.; Ying, W.; Zhiming, D.; Jianjun, Q.; Yi, S.; Shoujing, L. Enhancing room temperature mechanical properties of Mg–9Al–Zn alloy by multi-pass equal channel angular extrusion. *J. Mater. Process. Technol.* **2010**, *210*, 751–758.

12. Mallikarjuna, C.; Shashidhara, S.M.; Mallik, U.S. Evaluation of grain refinement and variation in mechanical properties of equalchannel angular pressed 2014 aluminum alloy. *Mater. Des.* **2009**, *30*, 1638–1642. [[CrossRef](#)]
13. Ramu, G.; Bauri, R. Effect of equal channel angular pressing (ECAP) on microstructure and properties of Al–SiCp composites. *Mater. Des.* **2009**, *30*, 3554–3559. [[CrossRef](#)]
14. Tham, Y.W.; Fu, M.W.; Hng, H.H.; Yong, M.S.; Lim, K.B. Bulk nanostructured processing of aluminum alloy. *J. Mater. Process. Technol.* **2007**, *192–193*, 575–581. [[CrossRef](#)]
15. Purcek, G. Improvement of mechanical properties for Zn–Al alloys using equal-channel angular pressing. *J. Mater. Process. Technol.* **2005**, *169*, 242–248. [[CrossRef](#)]
16. Saray, O.; Purcek, G. Microstructural evolution and mechanical properties of Al–40 wt.%Zn alloy processed by equal-channel angular extrusion. *J. Mater. Process. Technol.* **2009**, *209*, 2488–2499. [[CrossRef](#)]
17. Tolaminejad, B.; Dehghani, K. Microstructural characterization and mechanical properties of nanostructured AA1070 aluminum after equal channel angular extrusion. *Mater. Des.* **2012**, *34*, 285–292. [[CrossRef](#)]
18. Adedokun, S.T. A Review on Equal Channel Angular Extrusion as a Deformation and Grain Refinement Process. *J. Emerg. Trends Eng. Appl. Sci. (JETEAS)* **2011**, *2*, 360–363.
19. Javidikia, M.; Hashemi, R. Mechanical anisotropy in ultra-fine grained aluminium tubes processed by parallel-tubular-channel angular pressing. *Mater. Sci. Technol.* **2017**, *33*, 2265–2273. [[CrossRef](#)]
20. Mohammadtaheri, M. A New Metallographic Technique for Revealing Grain Boundaries in Aluminum Alloys. *Metallogr. Microstruct. Anal.* **2012**, *1*, 224–226. [[CrossRef](#)]
21. Rahimi, H.; Sedighi, M.; Hashemi, R. Forming limit diagrams of fine-grained Al 5083 produced by equal channel angular rolling process. *Proc. Inst. Mech. Eng. Part L J. Mater. Des. Appl.* **2018**, *232*, 922–930. [[CrossRef](#)]
22. Chung, Y.H.; Woo Park, J.; Lee, K.H. An analysis of accumulated deformation in the equal channel angular pressing (ECAP) process. *Metals Mater. Int.* **2006**, *12*, 289. [[CrossRef](#)]
23. Dieter, G.E. *Mechanical Metallurgy*; Bever, M.B., Copley, S.M., Shank, M.E., Wert, C.A., Wilkes, G.L., Eds.; McGraw-Hill Company (UK) Limited: London, UK, 1988; p. 280.
24. Baharanchi, M.A.; Karimzadeh, F.; Enayati, M.H. Mechanical and tribological behavior of severely plastic deformed Al6061 at cryogenic temperatures. *Mater. Sci. Eng. A* **2017**, *683*, 56–63. [[CrossRef](#)]
25. Fang, D.R.; Zhang, Z.F.; Wu, S.D.; Huang, C.X.; Zhang, H.; Zhao, N.Q.; Li, J.J. Effect of equal channel angular pressing on tensileproperties and fracture modes of casting Al–Cu alloys. *Mater. Sci. Eng. A* **2006**, *426*, 305–313. [[CrossRef](#)]
26. Eizadjou, M.; Talachi, A.K.; Manesh, H.D.; Janghorban, K. Slidingwear behavior of severely deformed 6061 aluminum alloy by accumulative roll bonding (ARB) process. *Mater. Sci. Forum* **2011**, *667–669*, 1107–1112.
27. Abd ElAal, M.I.; Um, H.Y.; Yoon, E.Y.; Kim, H.S. Microstructure evolution and mechanical properties of pure aluminumdeformed by equal channel angular pressing and direct extrusion in one step through an integrated die. *Mater. Sci. Eng. A* **2015**, *625*, 252–263. [[CrossRef](#)]
28. Xu, S.; Zhao, G.; Luan, Y.; Guan, Y. Numerical studies on processing routes and deformation mechanism ofmulti-pass equal channel angular pressing processes. *J. Mater. Process. Technol.* **2006**, *176*, 251–259. [[CrossRef](#)]